Invited paper

Magnetic correlations in a classic Mott system

Wei Bao[a],*, C. Broholm[b], G. Aeppli[c], S.A. Carter[d], P. Dai[e], C.D. Frost[f], J.M. Honig[g], P. Metcalf[g]

[a] *Brookhaven National Laboratory, Building 510B, Upton, NY 11973, USA*
[b] *The Johns Hopkins University, Baltimore, MD 21218, USA*
[c] *NEC, 4 Independence Way, Princeton, NJ 08540, USA*
[d] *University of California, Santa Cruz, CA 95064, USA*
[e] *Oak Ridge National Laboratory, Oak Ridge, TN 37831, USA*
[f] *ISIS, Rutherford Appleton Laboratory, Oxon, OX11 0QX, UK*
[g] *Purdue University, West Lafayette, IN 47907, USA*

Abstract

The metal-insulator transition in pure and doped V_2O_3 causes a fundamental change in its magnetism. While the antiferromagnetic insulator (AFI) is a Heisenberg localized spin system, the antiferromagnetism in the strongly correlated metal is determined by a Fermi surface instability. Paramagnetic fluctuations in the metal and insulator represent similar spatial spin correlations, but are unrelated to the long-range order in the AFI. The phase transition to the AFI induces an abrupt switching of magnetic correlations to a different magnetic wave vector. The AFI transition, therefore, is not a conventional spin order-disorder transition. Instead it is accounted for by an ordering in the occupation of the two degenerate d-orbitals at the Fermi level. © 1998 Elsevier Science B.V. All rights reserved.

Keywords: Mott localization; Spin density wave; Itinerant electrons – antiferromagnetism; Orbital ordering; Paramagnetic fluctuations

Some of the most fascinating members of strongly correlated electron systems are transition-metal oxides. For example, superconductivity occurs at a temperature as high as 133 K at ambient pressure in $HgBa_2Ca_2Cu_3O_{8+\delta}$ [1, 2]. Colossal magnetoresistance, where the resistivity is reduced by two orders of magnitude in a magnetic field of 6 T, is realized in (La, Y)MnO_3 [3]. In V_2O_3, the resistivity increases by eight orders of magnitude at a metal-insulator transition [4–6]. At this stage, our theoretical knowledge of strongly correlated systems is rather sketchy and fragmental. Accumulating empirical knowledge with experiments is indispensable. Since static or dynamic magnetic correlations are the natural consequences of strong Coulomb correlations and depend sensitively on electron wave functions, their direct measurement by neutron scattering can provide

fresh insight about the electronic processes. In this paper, such an endeavor for the classic Mott system, pure and doped V_2O_3 [7], is reviewed.

A composition-temperature phase diagram for V_2O_3 is presented in Fig. 1. The metal-insulator transition in the paramagnetic phase is a classic example of the Mott-Hubbard transition [8]. Metallic V_2O_3 is a strongly correlated Fermi liquid with a Sommerfeld specific-heat constant $\gamma = 54$–70 mJ/K^2 per mole V [9–11] and with a T^2 dependence of resistivity below ~ 40 K with a coefficient 0.30–0.05 $\mu\Omega$ cm/K^2 [12–14]. There is also long-range antiferromagnetic order in the doping-induced metal [15, 16].

The magnetic structure in the antiferromagnetic metal (AFM) was only recently determined by us using neutron diffraction [17]. It is a transverse incommensurate spin-density wave (SDW) with a staggered moment of 0.15 μ_B per vanadium (see Fig. 2). This small moment antiferromagnetic long-range order is accompanied by dynamic magnetic correlations with a bandwidth more than

* Corresponding author. Fax: + 1 516 344 2918; e-mail: bao@solids.phy.bnl.gov.
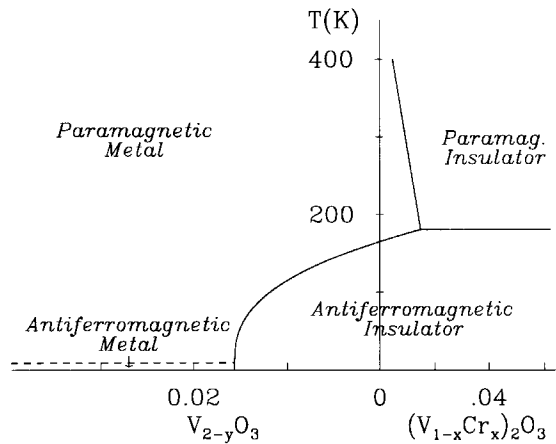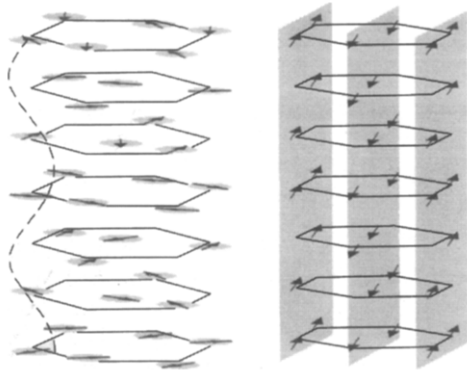
Fig. 2. (left) Magnetic structure in the SDW state of $V_{2-y}O_3$, from Ref. [17]. The incommensurate spiral has wave vector (0 0 1.7) using the conventional hexagonal unit cell shown here. (right) Magnetic structure in the AFI state of V_2O_3, according to Ref. [27]. The magnetic wave vector is $(\frac{1}{2}\frac{1}{2}0)$.

Fig. 3. Intensity contour of $S(q, \omega)$ along (1 0 l) direction at 1.4 K for $V_{1.973}O_3$ [29]. The q range spans a whole Brillouin zone with nuclear Bragg points (1 0 $\bar{2}$) and (1 0 4) at the ends. The two points at (1 0 $\overline{0.3}$) and (1 0 2.3) are magnetic Bragg points. Intensity is indicated by the bar on the right side in units of μ_B^2/meV per unit cell.

20 times $k_B T_N$ and an amplitude of more than 0.32 μ_B per vanadium, substantially larger than the ordered moment. Short-range magnetic correlations exist even at temperatures more than 20 times of the Néel temperature in the metal [18]. These results cannot be explained by localized spin models. Instead, they are analogous to the SDW in Cr metal [19]. However, in contrast to Cr, only a small area of the Fermi surface is involved in the SDW in metallic $V_{2-y}O_3$ [17], and strong electron correlations in metallic V_2O_3 require only near nesting of the Fermi surface for the SDW to occur.

Because of strong correlations, the Fermi velocity for metallic V_2O_3 is smaller than that for Cr metal by one order of magnitude [17]. This removes the problems in resolving the excitation spectrum which has plagued neu-
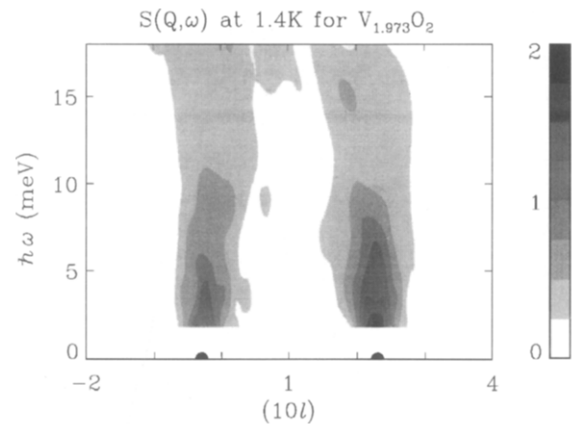
tron scattering studies of Cr. We have established unambiguously that the intrinsic dynamic spin correlation function, $S(q, \omega)$, even at 1.4 K in the ordered AFM phase, consists of a single broad lobe at each antiferromagnetic Bragg point in the energy range, 1.5 meV $\leqslant \hbar\omega \leqslant$ 25 meV, which we have probed [17, 20] (see Fig. 3). These broad lobes represent spin excitations inside the Stoner electron–hole continuum. Their dominance in spin dynamics reflects the fact that metallic V_2O_3 is in the small moment limit, in other words, it is near the quantum critical point for itinerant antiferromagnetism [18, 21, 22].

We have measured spin excitations throughout the Brillouin zone from 1.4 to 200 K for a metallic sample, $V_{1.973}O_3$ (T_N = 9 K) [18]. By normalizing to neutron scattering from transverse phonons, the dynamic spin correlation function, $S(q, \omega)$, was obtained in absolute units. We found that the q, ω and T dependence of spin fluctuations can be described by the self-consistent renormalization (SCR) theory for itinerant antiferromagnetism in the small moment limit [23–26]. Thermodynamic properties below $\sim 10T_N$ are quantitatively accounted for by this theory in its simplest form with four experimentally determined parameters [18].

Accompanied by a strongly *first-order* antiferromagnetic transition as well as a structural transition, the metal–insulator transition from the paramagnetic metal (PM) to the AFI is considerably more complex than the metal–insulator transition in the paramagnetic phase. The mechanism for this phase transition has been controversial. We examined the PM–AFI transition by investigating the spin dynamics of a pure V_2O_3 sample. The
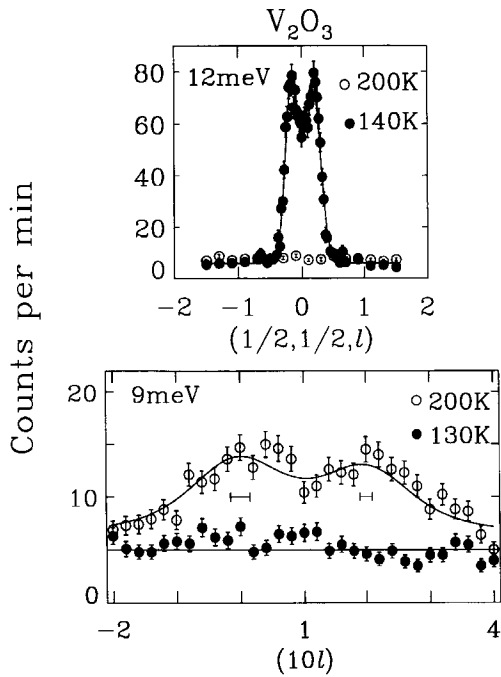
Fig. 4. Constant $\hbar\omega$ scan along $(\frac{1}{2}\,\frac{1}{2}\,l)$ (upper panel) and $(1\,0\,l)$ (lower panel) in the PM (open circles) and the AFI (solid circles) phases for V_2O_3, from Ref. [29].
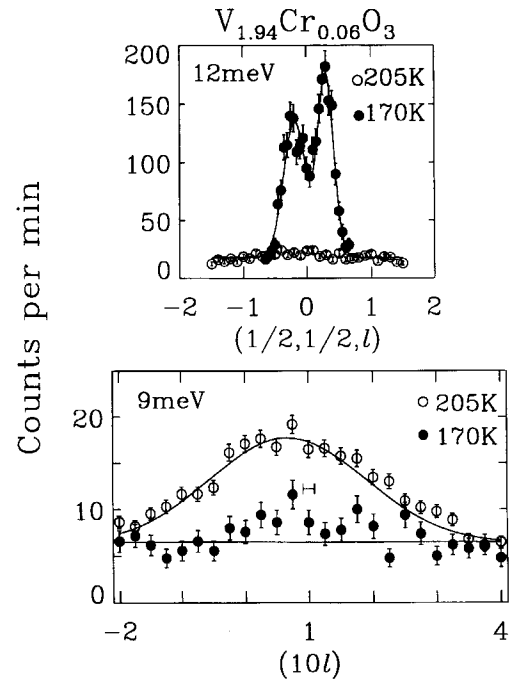
Fig. 5. Constant $\hbar\omega$ scan along $(\frac{1}{2}\,\frac{1}{2}\,l)$ (upper panel) and $(1\,0\,l)$ (lower panel) in the PI (open circles) and the AFI (solid circles) phases for $V_{1.94}Cr_{0.06}O_3$, from Ref. [29].

magnetic structure in the AFI [27] is composed of vertical ferromagnetic planes whose spin direction alternates with a wave vector in the basal plane (see Fig. 2). Magnetic excitations are conventional spin waves [20, 28] and magnetism *inside* the AFI phase can be accounted for by a conventional Heisenberg localized spin model. The antiferromagnetic transition, however, is not conventional. In the upper panel of Fig. 4, the two counterpropagating spin-wave modes are shown by solid circles at 140 K in the AFI phase. When the sample is in the PM phase at 200 K, there is no critical scattering present as shown by the open circles. The magnetic correlations in the PM-phase change to yield neutron scattering which peaks at the Bragg points for the SDW (refer to open circles in the lower panel). In the AFI phase, there are no magnetic correlations of the SDW type as shown by the solid circles at 130 K. The PM–AFI transition, therefore, is accompanied by an abrupt switching between two different kinds of magnetic correlations (see Refs. [20, 29] for details).

The paramagnetic spin fluctuations in the insulator (PI) also have different spatial correlations from those in the low-temperature AFI phase, as shown in Fig. 5 for a Cr-doped V_2O_3 sample. Similar to those in the PM, they peak in a region of q-space displaced from nuclear Bragg points along the c-axis (refer to the $(1\,0\,l)$ scan in the lower panel). Similar switching of magnetic correla-

tions occurs at the PI–AFI phase transition [20, 29]. Thus, the magnetic transition from either the PM or the PI to the AFI is not a conventional spin order–disorder transition, rather it appears that the spin Hamiltonian is abruptly altered by an underlying phase transition.

There are other anomalies in the dynamic spin correlations of the PI. As is evident from the broader peak width of constant-E scans in the PI as compared to the PM (refer to the $(1\,0\,l)$ scans in Figs. 4 and 5), the correlation length in the PI is even shorter than that for the PM where electron-hole damping exists. This short correlation length amounts only to a nearest-neighbor distance and shows no discernible increase as the AFI transition is approached by cooling the sample [20]. Nevertheless, these extremely short-range dynamic magnetic correlations involve a substantial magnetic moment, 0.81 μ_B per V, below 18 meV at 205 K. Therefore, they are not due to weak magnetic interactions ($J \ll k_B T$).

All these results can be consistently explained, as pointed out by Rice [30], by considering the doubly degenerate d-orbitals at the Fermi level for each electron on a vanadium site. It has been shown more than 20 years ago that the extra degrees of freedom from orbital degeneracy have a profound effect on the Hubbard physics [31–33]. Specifically, the spin and orbital degrees of freedom strongly influence each other. In the AFI phase of V_2O_3, spin-order develops simultaneously

with order in the orbital occupations at V sites [33]. In the PI phase, orbital occupations fluctuate [30], thereby inducing magnetic interactions with fluctuating signs. It is no wonder then that dynamic spin correlations in the PI are of large amplitude and yet remain extremely short-ranged [20, 29]. This is very different from the one-band case where insulating antiferromagnetism is described by a fixed Heisenberg spin Hamiltonian [34]. It would be interesting to study the localized spin systems with fluctuating exchange interactions, and details of our experimental results in the PI remain to be understood [20].

In summary, the metal–insulator transition fundamentally alters the nature of antiferromagnetism in the system V_2O_3. Contrary to widely circulated beliefs, the magnetism is itinerant in nature and is still determined by the Fermi sea in the nearly localized Fermi liquid of metallic V_2O_3. The first-order AFI transition is primarily an orbital-ordering transition. Strong spin–orbital coupling results from different overlap integrals between anisotropic d-orbitals on neighboring sites.

References

[1] A. Schilling, M. Cantoni, J.D. Guo, H.R. Ott, Nature 363 (1993) 56.
[2] Z.J. Huang et al., Physica C 217 (1993) 1.
[3] S. Jin, H.M. O'Bryan, T.H. Tiefel, M. McCormack, W.W. Rhodes, Appl. Phys. Lett. 66 (1995) 382.
[4] J. Feinleib, W. Paul, Phys. Rev. 155 (1967) 841.
[5] M. Föex, Compt. Rend. 223 (1946) 1126.
[6] F.J. Morin, Phys. Rev. Lett. 3 (1959) 34.
[7] N.F. Mott, Metal–Insulator Transitions, 2nd ed, Taylor and Francis, London, 1990.
[8] D.B. McWhan, T.M. Rice, J.P. Remeika, Phys. Rev. Lett. 23 (1969) 1384.
[9] D.B. McWhan, J.P. Remeika, T.M. Rice, W.F. Brinkman, J.P. Maita, A. Menth, Phys. Rev. Lett. 27 (1971) 941.
[10] D.B. McWhan, J.P. Remeika, J.P. Maita, H. Okinaka, K. Kosuge, S. Kachi, Phys. Rev. B 7 (1973) 326.
[11] S.A. Carter, T.F. Rosenbaum, P. Metcalf, J.M. Honig, J. Spalek, Phys. Rev. B 48 (1993) 16841.
[12] D.B. McWhan, T.M. Rice, Phys. Rev. Lett. 22 (1969) 887.
[13] D.B. McWhan, A. Menth, J.P. Remeika, W.F. Brinkman, T.M. Rice, Phys. Rev. B 7 (1973) 1920.
[14] Y. Ueda, K. Kosuge, S. Kachi, J. Solid State Chem. 31 (1980) 171.
[15] Y. Ueda, K. Kosuge, S. Kachi, T. Shinjo, T. Takada, Mater. Res. Bull. 12 (1977) 87.
[16] J. Dumas, C. Schlenker, J. Magn. Magn. Matter. 7 (1978) 252.
[17] W. Bao, C. Broholm, S.A. Carter, T.F. Rosenbaum, G. Aeppli, S.F. Trevino, P. Metcalf, J.M. Honig, J. Spalek, Phys. Rev. Lett. 71 (1993) 766.
[18] W. Bao, C. Broholm, J.M. Honig, P. Metcalf, S.F. Trevino, Phys. Rev. B 54 (1996) R3726.
[19] E. Fawcett, Rev. Mod. Phys. 60 (1988) 209.
[20] W. Bao, C. Broholm, G. Aeppli, S.A. Carter, P. Dai, T.F. Rosenbaum, J.M. Honig, P. Metcalf, S.F. Trevino, 1997 to be published.
[21] A.J. Millis, Phys. Rev. B 48 (1993) 7183.
[22] S. Sachdev, J. Ye, Phys. Rev. Lett. 69 (1992) 2411.
[23] T. Moriya, K. Ueda, J. Phys. Soc. Japan 63 (1994) 1871.
[24] K. Nakayama, T. Moriya, J. Phys. Soc. Japan 56 (1987) 2918.
[25] H. Hasegawa, J. Phys. Soc. Japan 38 (1975) 107.
[26] H. Hasegawa, T. Moriya, J. Phys. Soc. Japan 36 (1974) 1542.
[27] R.M. Moon, Phys. Rev. Lett. 25 (1970) 527.
[28] R.E. Word, S.A. Werner, W.B. Yelon, J.M. Honig, S. Shivashankar, Phys. Rev. B 23 (1981) 3533.
[29] W. Bao, C. Broholm, G. Aeppli, P. Dai, J.M. Honig, P. Metacalf, Phys. Rev. Lett. 78 (1997) 507.
[30] T.M. Rice, in: A. Fujimori, Y. Tokura (Eds.), Spectroscopy of Mott Insulators and Correlated Metals, Springer, Berlin, 1995.
[31] K.I. Kugel, D.I. Khomskii, Sov. Phys.-JETP 37 (1973) 725.
[32] M. Cyrot, C. Lyon-Caen, J. Phys. (Paris) C 4 (1976) 183.
[33] C. Castellani, C.R. Natoli, J. Ranninger, Phys. Rev. B 18 (1978) 4945.
[34] P.W. Anderson, Solid State Phys. 14 (1963) 99.